

Decoding Topological Subsystem Color Codes Over the Erasure Channel using Gauge Fixing

Hiteshvi Manish Solanki and Pradeep Kiran Sarvepalli

Department of Electrical Engineering, Indian Institute of Technology Madras, Chennai 600 036, India

(Dated: April 18, 2022)

Topological subsystem color codes (TSCCs) are an important class of topological subsystem codes that allow for syndrome measurement with only 2-body measurements. It is expected that such low complexity measurements can help in fault tolerance. While TSCCs have been studied over depolarizing noise model, their performance over the erasure channel has not been studied as much. Recently, we proposed erasure decoders for TSCCs and reported a threshold of 9.7%. In this paper, we continue our study of TSCCs over the erasure channel. We propose two erasure decoders for topological subsystem color codes. These decoders use the technique of gauge fixing where some of the gauge operators of the subsystem code are promoted to stabilizers. We perform gauge fixing using 4-body and 8-body gauge operators. With partial gauge fixing we obtained a threshold of 17.7% on a TSCC derived from the square octagon lattice. Using an order maximal gauge fixing decoder we were able to improve the threshold to 44%. The previously known decoder for TSCC over the erasure channel had a threshold of 9.7%. We also study the correctability of erasures on the subsystem codes.

I. INTRODUCTION

Subsystem codes are an important generalization of stabilizer codes [1–3]. One of the motivations for this generalization was to simplify the error recovery process of quantum codes. Specifically, they can simplify the syndrome computation which involves the measurement of the stabilizer generators. These codes are defined by a (non-Abelian) subgroup of Pauli group called the gauge group. Of particular interest are the codes with local gauge group. Topological subsystem color codes are a class of subsystem codes where generators of the gauge group as well the stabilizer of the code are local.

The advantages of topological subsystem codes (TSCs) motivated many researchers to look at their performance under different noise models. Most of the studies on the performance of TSCs [4–7] focused on the depolarizing channel. The error correcting capabilities of TSCCs for handling leakage errors were explored in [8]. In contrast, the performance of TSCCs over the quantum erasure channel [9], which can be used to model qubit loss, has not been studied as much. Motivated by this gap, we began the study of topological subsystem color codes over the erasure channel and reported some preliminary results in [10]. Therein we proposed multiple two-stage erasure decoders for the TSCC derived from the square octagon lattice. Using a combination of various techniques like peeling and clustering we were able to achieve a threshold of 9.7% in [10] for the TSCC derived from the square octagon lattice. However, this threshold was not optimal and there was room for improvement.

In this paper, we continue our study of TSCCs over the erasure channel and present new decoding algorithms that improve upon the decoders in [10]. A driving force for this work is to improve the threshold of the TSCCs for erasure noise. Topological subsystem color codes have fewer stabilizer generators than a comparable color code or a surface code. This will lead to lower thresholds [4, 5, 11]. To address this we use the technique of gauge fixing, wherein we promote some of the gauge operators to checks. Gauge fixing in effect leads to a larger stabilizer. This technique of promoting some gauge operators to stabilizers was used for analyzing the structure of subsystem codes in [4], and for quantum computation in

[12, 13]. More recently, it was also employed for decoding subsystem codes [7].

An immediate question for the gauge fixing decoders is to determine which gauge operators to promote to stabilizers. We propose two decoding algorithms each of which makes a different choice of the operators for gauge fixing. Both of them rely on the fact that a TSCC can be mapped to color codes. Furthermore, the stabilizers of these color codes are in the gauge group of the TSCC. We choose two different sets of these color code stabilizers for gauge fixing.

Another question in the context of gauge fixing decoders is related to the sequence of measurement of the gauge operators. In our case, all the gauge operators that we promote to stabilizers anticommute with some 2-body gauge operator of the TSCC. While we were able to obtain efficient decompositions of these additional stabilizers individually, these decompositions were not amenable to a joint measurement using 2-body measurements. Therefore our decoding algorithms require direct measurement of these stabilizers. Then employing the mapping of the TSCC to color codes, we proceed to decode the TSCC.

We briefly summarize our main contributions below.

- (i) First, we propose a decoder that uses partial gauge fixing for TSCC. We obtain a threshold of 17.7% for TSCC derived from the square octagon lattice.
- (ii) We then propose an alternate “order” maximal gauge fixing decoder to improve the threshold. This decoder leads to a threshold of threshold 44%. This improvement is attained at the expense of a slight increase in complexity.
- (iii) We study the correctability of erasures on a subsystem code. Specifically, we provide a necessary and sufficient condition for an erasure pattern to be correctable on a subsystem code (without gauge fixing). We also study correctability of erasures under the order maximal gauge fixing decoder.

There are two related works in addition to our previous work [10]. In [8], the authors studied topological subsystem codes for correcting leakage errors, a more severe form of noise than erasure noise. While somewhat related, this noise model is different from ours and assumes that the locations of the erased qubits are unknown. With respect to the tech-

nique of gauge fixing, the closest work is that of [7] where the authors also use gauge fixing for decoding subsystem codes. They studied subsystem surface codes and their generalizations over hyperbolic surfaces under depolarizing noise and biased noise models.

We organize the paper as follows. In Section II we review the background for our proposed decoders. In Section III we give an overview of the proposed decoding algorithms. Section IV elaborates on syndrome measurement and preprocessing techniques. In Section V we discuss the first stage for X error correction and in Section VI the second stage for Z error correction. Then we study conditions for correctability of erasures on subsystem codes in Section VII. We report the simulation results in Section VIII and finally conclude with a brief summary in Section IX.

In the previous version of this paper, we incorrectly claimed that the additional operators for gauge fixing can be jointly measured using 2-body and 4-body operators. This claim has been withdrawn in this version. We thank Oscar Higgot for pointing out the error.

II. BACKGROUND

In this section, we briefly review some background material. We assume that the reader is familiar with stabilizer codes, see [14, 15] for an introduction.

A. Subsystem codes

We briefly review subsystem codes. For more details we refer the reader to [15]. Subsystem codes are obtained from stabilizer codes by not encoding information in some of the logical qubits. These qubits are called the gauge qubits. Any error on the gauge qubits do not affect the codespace. An $[[n, k, r, d]]$ subsystem code encodes k logical qubits and r gauge qubits into n qubits. It can detect errors upto $d - 1$ qubits, where d is the distance of the code. The distance also signifies the smallest weight of non-trivial logical operator.

We define a subsystem code by a subgroup $\mathcal{G} \subset \mathcal{P}_n$, where \mathcal{P}_n is the Pauli group on n qubits. Elements of \mathcal{G} are called the *gauge operators*. Elements which generate the gauge group are called the *gauge generators*. Recall that the centralizer of a subgroup $\mathcal{G} \subseteq \mathcal{P}_n$ is defined as

$$C(\mathcal{G}) = \{g \in \mathcal{P}_n \mid gh = hg \text{ for all } h \in \mathcal{G}\} \quad (1)$$

The *stabilizer* \mathcal{S} of the subsystem code is a subgroup of \mathcal{G} such that $\langle iI, \mathcal{S} \rangle = \mathcal{G} \cap C(\mathcal{G})$, where $C(\mathcal{G})$ is the centralizer of \mathcal{G} . Elements of \mathcal{S} act trivially on the code space. It is convenient to ignore the phases and write the stabilizer up to a phase as follows.

$$\mathcal{S} = \mathcal{G} \cap C(\mathcal{G}) \quad (2)$$

Since $\mathcal{S} \subseteq \mathcal{G}$, it follows that

$$\mathcal{S} \subseteq \mathcal{G} \subseteq C(\mathcal{G}) \subseteq C(\mathcal{S}). \quad (3)$$

For an $[[n, k, r, d]]$ subsystem code, ignoring phases, there are $2r + s$ independent generators for \mathcal{G} and s independent generators for \mathcal{S} , where $n = k + r + s$, see [3]. Operators in $C(\mathcal{G}) \setminus \mathcal{G}$ are called bare logical operators while operators in $C(\mathcal{S}) \setminus \mathcal{G}$, obtained by appending gauge operators to the bare logical operators, are called dressed logical operators, see [5].

B. Topological color codes

Topological color codes (TCCs) in 2D are defined on lattices where the vertices are trivalent and faces are 3-colorable [16]. These lattices are also called 2-colexes. A quantum code can be defined on 2-colex by placing qubits on the vertices, and checks on faces. (We can shall refer to a 2-colex as a color code for this reason). For any face f , a pair of stabilizers are defined as follows:

$$B_f^X = \prod_{v \in f} X_v \text{ and } B_f^Z = \prod_{v \in f} Z_v \quad (4)$$

where X and Z are the Pauli matrices. Let F_γ be set of faces of γ color, $\gamma \in \{r, g, b\}$. These checks satisfy the following relations:

$$\prod_{f \in F_r} B_f^Z = \prod_{f \in F_g} B_f^Z = \prod_{f \in F_b} B_f^Z \quad (5a)$$

$$\prod_{f \in F_r} B_f^X = \prod_{f \in F_g} B_f^X = \prod_{f \in F_b} B_f^X \quad (5b)$$

This equality depicts that there are four dependencies among the stabilizer generators given in Eq. (4). A color code defined on a 2-colex embedded on a surface of genus g encodes $4g$ qubits. For the rest of the paper we assume that the color code is defined on a torus which has genus one. In this case the color code encodes 4 logical qubits.

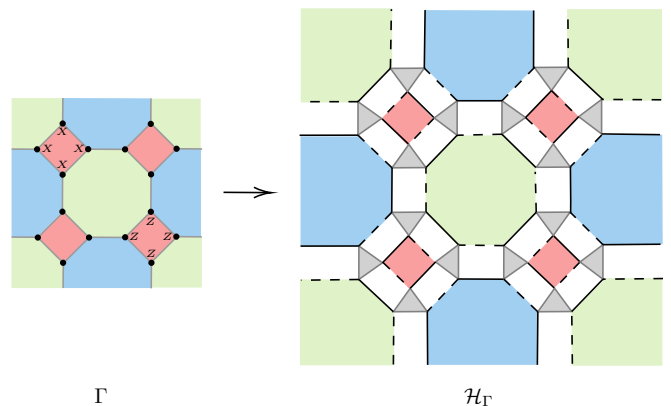


FIG. 1: The figure on left shows the color code defined on 2-colex. Solid dots indicate the qubits. Every face has a X type stabilizer and a Z type stabilizer associated to it. A hypergraph \mathcal{H}_Γ can be constructed from this 2-colex. The hypergraph is depicted on the right. Shaded triangles correspond to rank-3 edges. A TSCC is defined on this hypergraph. Qubits are located on the vertices of the hypergraph and its edges define the gauge group of the TSCC as in Eq. (7).

C. Topological subsystem color codes

Topological subsystem color codes (TSCCs) are a class of subsystem codes obtained from TCCs [17]. To construct a TSCC, we construct a hypergraph from the 2-colex on which the color code is defined. Recall that the hypergraph is defined by an ordered pair (V, E) where V is the set of vertices of the hypergraph and E , called edges of the hypergraph, is a collection of subsets of V . First, we replace every TCC vertex with a triangle. The three vertices of triangle form a rank-3 edge. If u, v, w are the vertices of the triangle, then the corresponding rank-3 edge is denoted (u, v, w) . These newly formed vertices are denoted V . Next we split every edge to two edges: solid and dashed, placed in alternating fashion around each triangle, see Fig. 1. These newly formed edges are called rank-2 edges. The resulting object is a hypergraph as shown in [5]. The collection of rank-2 edges is denoted E_2 while the set of rank-3 edges is denoted E_3 . Together they constitute $E = E_2 \cup E_3$, the edges of the hypergraph. The hypergraph is now defined by the ordered pair (V, E) .

Faces are somewhat more complicated to define. Each face of the color code gives rise to a face in the hypergraph. It also inherits the color from the underlying face in the 2-colex. We denote these faces by F . The c colored faces are denoted F_c . Note that $F = F_r \cup F_g \cup F_b$.

One can construct a subsystem code from the hypergraph obtained from the 2-colex as follows, see [5, 17]. Place qubits on the vertices of the hypergraph and for each rank-2 edge of the hypergraph we associate a Pauli operator. Every rank-3 edge $e = (u, v, w)$ is also assigned an operator $K_e = Z_u Z_v Z_w$. Note that for each rank-3 edge (u, v, w) we define three ZZ operators for each pair of vertices, namely, $Z_u Z_v$, $Z_v Z_w$ and $Z_u Z_w$. Of these three ZZ operators only two are independent. These 2-body ZZ operators along with the rank-2 edge operators generate the gauge group of the TSCC. (Note that the operator $Z_u Z_v Z_w$ is not a gauge operator.) If a pair of vertices $e = (u, v)$ form a rank-2 edge or belong to a rank-3 edge we define

$$K_e = K_{(u,v)} = \begin{cases} X_u X_v & (u, v) \text{ is dashed edge} \\ Y_u Y_v & (u, v) \text{ is solid edge} \\ Z_u Z_v & (u, v) \text{ is in some hyperedge} \end{cases} \quad (6)$$

We can then define the gauge group of the subsystem code as follows.

$$\mathcal{G} = \langle K_{(u,v)} \mid (u, v) \text{ are adjacent} \rangle \quad (7)$$

The stabilizers and the logical operators of the TSCC are completely determined by the gauge group. In case of TSCCs, they can be characterized in terms of cycles of the hypergraph.

A cycle in a hypergraph is a collection of edges such that every vertex has an even degree with respect to these edges. A rank-2 cycle involves only rank-2 edges. A hypercycle involves both rank-2 edges and hyperedges (rank-3 edges). To every cycle σ we can associate an operator as follows.

$$W(\sigma) = \prod_{e \in \sigma} K_e \quad (8)$$

The importance of these operators is that they are precisely the operators in $C(\mathcal{G})$, the centralizer of \mathcal{G} . A generating set for $C(\mathcal{G})$ can be given by considering all the cycles. Cycles of trivial homology generate the stabilizer of the TSCC, as shown in Fig. 2. Cycles of nontrivial homology give rise to the logical operators of the TSCC.

For every face $f \in F$, we associate two independent cycles:

- i) A rank-2 cycle denoted σ_1^f . This is formed by the rank-2 edges in the boundary of f .
- ii) A hypercycle denoted σ_2^f . This is formed by the rank-2 as well as rank-3 edges in the boundary of f .

(A dependent hypercycle can be generated by σ_1^f and σ_2^f .) The hypercycle σ_2^f is chosen so that the edges corresponding to the XX type gauge operators in the boundary of f are chosen to be in the hypercycle, see Fig. 2. Cycles of trivial homology correspond to stabilizer generators of the subsystem code. We denote the stabilizer from rank-2 cycles as W_1^f and the stabilizer from the hypercycle as W_2^f .

$$W_1^f = \prod_{e \in \sigma_1^f} K_e = \prod_{v \in f} Z_v \quad (9a)$$

$$W_2^f = \prod_{e \in \sigma_2^f} K_e = \prod_{(u,v,w) \in f} X_u Y_v Y_w, \quad (9b)$$

where K_e is the edge operator associated to the edge e . The alternate forms simply follow by substituting for the edge operators K_e . Fig. 2 shows these stabilizers: W_1 on faces f_1 and f_2 and W_2 on faces f_3 and f_4 .

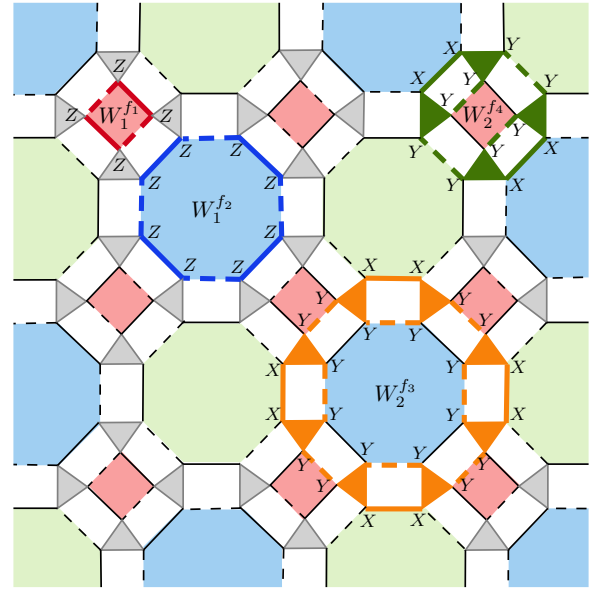


FIG. 2: Subsystem code defined on square octagon lattice. Also shown are the cycles and the associated stabilizers (in color). Every face has a Z type stabilizer coming from the rank-2 cycle, see $W_1^{f_1}$ and $W_1^{f_2}$. Every face also has a stabilizer attached to a hypercycle, see $W_2^{f_3}$ and $W_2^{f_4}$. This stabilizer is neither X type nor Z type.

The following dependencies exist among the stabilizer generators of the topological subsystem color codes on a torus.

$$\prod_{f \in F_r} W_2^f \prod_{f \in F_g} W_2^f = \prod_{f \in F_b} W_1^f \prod_{f \in F_r} W_1^f \quad (10a)$$

$$\prod_{f \in F_r} W_2^f \prod_{f \in F_b} W_2^f = \prod_{f \in F_g} W_1^f \prod_{f \in F_b} W_1^f \quad (10b)$$

The above relations show that there are $s = 2|F| - 2$ independent stabilizer generators for the TSCC assuming that there are $|F|$ faces.

Remark 1. When defined on a torus we can show that the number of qubits is $n = 6|F|$. The number of independent gauge generators is given by $2r + s = 10|F| - 2$, where r is the number of gauge qubits which gives us $r = 4|F|$. The number of encoded qubits is $k = 2$.

D. Mapping a TSCC onto color codes

Ref. [4] proposed a mapping of subsystem codes onto three copies of color codes. We illustrate this in Fig. 3, for the TSCC derived from the square octagon lattice. The faces of the TSCC are colored with three different colors. Qubits belonging to faces of same color are grouped together and all of them are colored the same. Each of this stack (group) of qubits can be reinterpreted as a color code, see Fig. 3. This mapping could be viewed as a reinterpretation of the operators on the subsystem code in terms of these copies of color codes.

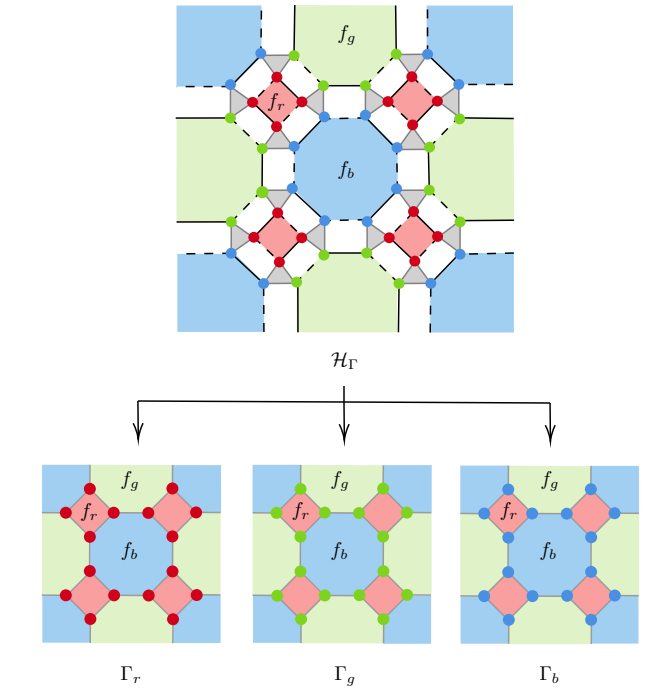


FIG. 3: Faces of TSCC are colored in red, green and blue. Qubits are highlighted with the color of the face they belong to. Every stack of qubits of same color form a color code identical to the parent color code of the TSCC. The faces in each stack are labeled same as the parent face in the hypergraph.

In mapping a TSCC to three copies of the parent TCC, we extend the stabilizer of the subsystem code to $\mathcal{S}_e \subseteq \mathcal{G}$, where \mathcal{S}_e is generated by all the stabilizers of the three copies of the parent color code. Therefore, we have

$$\mathcal{S} \subseteq \mathcal{S}_e \subseteq \mathcal{G} \subseteq C(\mathcal{G}) \subseteq C(\mathcal{S}_e) \subseteq C(\mathcal{S}). \quad (11)$$

Note that \mathcal{S}_e is an Abelian group. There exist other ways to map a TSCC onto color codes, see [4, 6].

E. Error model

We assume the erasures occur independently on each qubit with a probability ε and each qubit is erased with probability ε . Once the loss is detected, the erased qubit is replaced with a completely mixed state. For the purposes of decoding, we can measure the syndrome with the replaced qubit [18–21]. Since the completely mixed state can be written as $\frac{I}{2} = \frac{1}{4}\rho + \frac{1}{4}X\rho X + \frac{1}{4}Y\rho Y + \frac{1}{4}Z\rho Z$ this is equivalent to placing one of the Pauli errors, I, X, Y, Z with equal probability on the erased qubit. These errors are induced by the erasure and we refer to them as erasure induced Pauli errors. Decoding over an erasure channel requires us to correct the erasure induced Pauli errors.

III. OVERVIEW OF THE GAUGE FIXING DECODERS

In this section we give an overview of proposed erasure decoders for TSCCs. As discussed in the previous section, for correcting the erasure errors, we can map them to Pauli errors on the erased qubits where each Pauli error occurs with equal probability. Although TSCCs are not CSS type codes, we can still correct these induced X and Z errors separately as in the case of the decoders proposed for the depolarizing channel [5, 6]. The proposed decoders have two stages: one for correcting X errors and one for correcting Z errors.

For the proposed decoders we map TSCC to three color code copies (refer Section IID) and decode over the color codes instead of decoding on the TSCC directly. Decoding by mapping onto the color codes implies that we augment the stabilizer by additional operators from the gauge group. We refer to this as gauge fixing since normally they are not constrained. However, in the proposed decoders they are also measured and treated as stabilizers. (Note that the 2-body gauge generators are not treated as stabilizers.) We propose two decoders which differ in how the phase flip errors are corrected.

For the first decoder, bit flip errors are corrected by mapping the TSCC onto three copies of color codes. This requires additional gauge operators corresponding to the Z type stabilizers of the color codes to be measured. These are used only for correcting the bit flip errors. After the bit flip errors are corrected the phase flip errors are corrected. The Z errors are corrected using the stabilizers of the subsystem code (hypercycle stabilizers). The phase flip errors are corrected by mapping TSCC to the parent color code from which the subsystem color code was derived. We refer to this decoder as the *partial gauge fixing decoder*.

For the second decoder, the bit flip errors are corrected as in the first decoder. In addition, the phase flip errors are also corrected by mapping them to color codes as in case of bit flip errors. This uses the X type stabilizers of the color codes also. These are used for correcting the phase flip errors. The stabilizers of the subsystem code corresponding to the hypercycles are not used directly in this decoder. The total number of gauge operators that are promoted to stabilizers is almost close to the maximal set possible. We refer to this as *order maximal gauge fixing decoder*. However, this additional complexity leads to an improvement in performance as will be seen later in Section VIII.

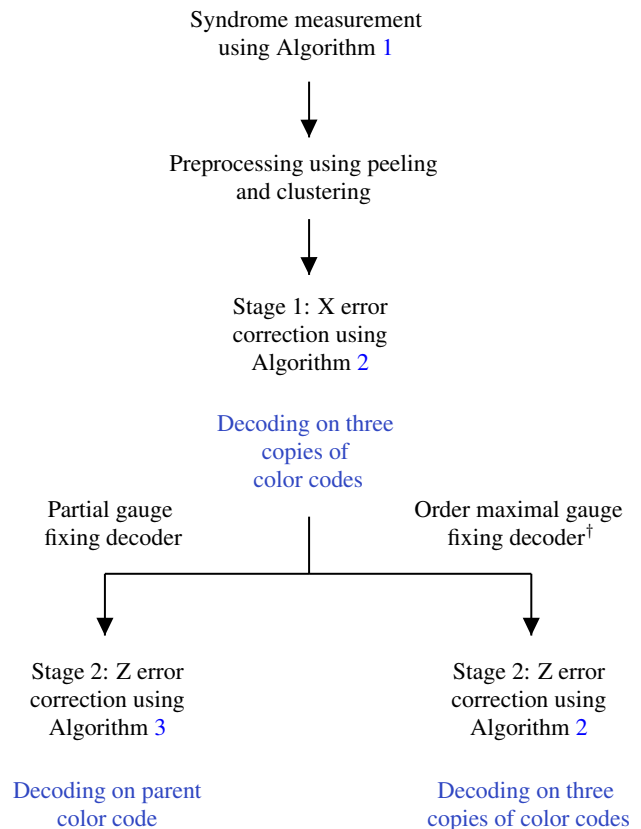


FIG. 4: Overview of proposed two stage subsystem decoders over the erasure channel. [†]For the second decoder, the order of Stage 1 and Stage 2 can be swapped or implemented parallelly.

A. Gauge fixing

In mapping the subsystem code to the color codes, the stabilizer of the subsystem code is extended to a larger stabilizer. This leads to gauge fixing where some of the gauge operators are promoted to checks [22]. Since our original code is a subsystem code, and we plan to decode it using the three stacks of color codes, a careful counting of the stabilizers on the color codes leads to the following observations. First of all the code we are interested in decoding is the subsystem code. This subsystem code has $2|F|$ stabilizer generators, with two dependencies. On the other hand mapping the subsystem color code to color code requires us to use $2|F|$ generators for each color code i.e. $6|F|$ stabilizer generators. (For correcting the X type errors we only need $3|F|$ syndromes and for correcting the phase flip errors $3|F|$). This means that we must be able generate additional “syndromes” on the color codes consistently. This naturally leads us to the idea of gauge fixing where in addition to the stabilizer generators of the subsystem code, we also measure some additional commuting set of gauge operators.

To obtain the additional syndromes on the color codes, we measure them directly on TSCC. We further show that there exists a decomposition of the color code stabilizers in smaller body gauge generator measurements, but measure-

ment of these individual gauge generators may not be possible due to their anticommuting nature.

We summarize the key requirements on the measurement of syndromes for the proposed decoders in light of the above discussion on gauge fixing.

- M1. Completeness: In order that the syndromes of the color codes are generated from the gauge measurements, we also require that all their stabilizers be generated gauge operators.
- M2. Locality: From the point of view of fault tolerance we want the stabilizers of color codes should also be measured locally on the TSCC.
- M3. Sequencing: Any gauge operator to be measured must commute with the product of previously measured gauge operators.

IV. SYNDROME MEASUREMENT AND PREPROCESSING

A popular approach for decoding topological codes is to map the original code into some other quantum code for which efficient decoders are known [4, 23–26]. For our decoding algorithm, we use the map discussed in Sec. IID. Instead of correcting errors on the TSCC, we correct the copies of color codes and then lift the error to subsystem code. In Sec. IVA we discuss the measurement for TCC and TSCC stabilizers. In Sec. IV B we discuss the preprocessing techniques to do before the actual decoding steps.

A. Measurement of TCC and TSCC stabilizers

We map the TSCC onto three (identical) copies of color codes. Our plan is to decode on the color codes instead on decoding on the TSCC. For this we need to measure the color code stabilizers on the TSCC.

One idea to reduce the complexity of the measurements of color coder stabilizers is to break them down to smaller body measurements (product of gauge generators). This is similar to how a TSCC stabilizer is measured using measurements of commuting gauge generators and then combining their outcome. Fig. 5 illustrates how the Z type stabilizers on the red stack can be decomposed as product of gauge generators. We can obtain similar map for X type stabilizers. Measurement of all these operators using only 2 body gauge generators is not possible since they anticommute among each other. Fig. 6 shows an example of how two gauge generators of stabilizers $B_{f_r}^X$ and $B_{f_g}^Z$, on the red stack, anticommute with each other at the highlighted location. Due to this, both the stabilizers cannot be measured simultaneously using the 2-body gauge operators[27].

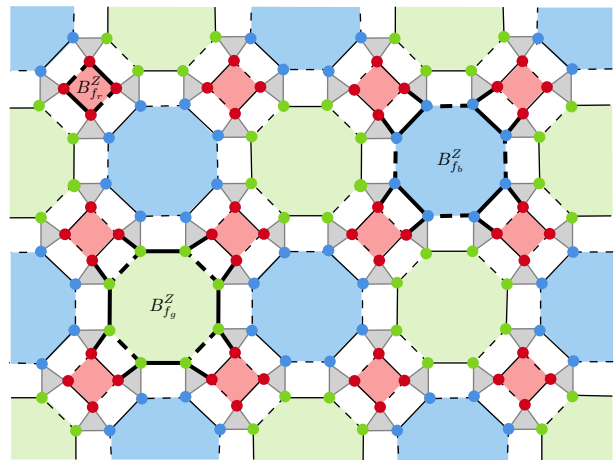


FIG. 5: Bold edges on the TSCC denote the 2-body decomposition for $B_{f_r}^Z$, $B_{f_b}^Z$ and $B_{f_g}^Z$ stabilizers for color code on red stack.

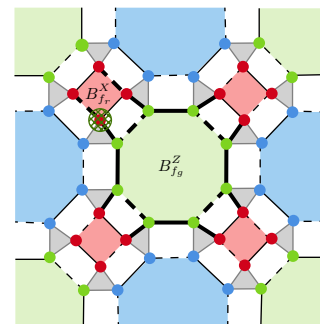


FIG. 6: Bold edges on the TSCC denote the 2-body decomposition for $B_{f_r}^X$ and $B_{f_g}^Z$ stabilizers for color code on red stack. The highlighted green net patterned circle shows the qubit where the 2-body XX gauge generator and the 2-body ZZ gauge generator anticommute.

Hence instead of measuring the color code stabilizer using product of individual gauge generators, we measure 4-body or 8-body TCC stabilizer directly on TSCC. Fig. 7 shows how these measurements are done on the TSCC to obtain the Z type color code stabilizers on red stack.

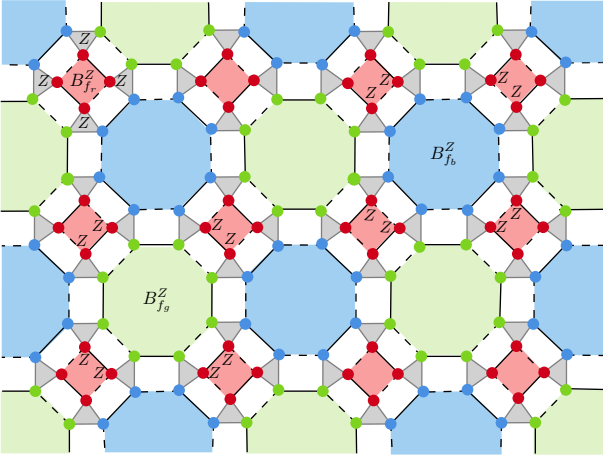


FIG. 7: Direct measurement of 4-body $B_{f_r}^Z$ stabilizer and 8-body $B_{f_b}^Z$ and $B_{f_g}^Z$ stabilizers for color code on red stack.

Similarly, we can directly measure both X type and Z type stabilizers, for all three stacks, on the TSCC using 4 and 8-body measurements. Note that while measuring stabilizers for c stack, where $c \in \{r, g, b\}$, only the qubits on c face of TSCC are involved.

Remark 2. Note that all the stabilizer generators of the color codes on each of the three stacks are generated as elements of the gauge group of the TSCC. The dependencies among the individual color codes are respected by this decomposition. So for instance on the color code on each stack the dependencies corresponding to Eq. (5a) are also respected.

The above remark makes sure that we get the correct measurement outcome for all the stabilizers after the syndrome measurement process. The syndrome measurement is given in Algorithm 1.

Observe that every W_1^f stabilizer corresponds to a color code stabilizer. In fact, $(B_f^Z)_c = W_1^f$ where $f \in F_c$. On the other hand, none of the color code stabilizer directly corresponds to the hypercycle stabilizer W_2^f of TSCC since W_2^f have support on all three stacks. However, the hypercycle stabilizer W_2^f can be decomposed into three stabilizers each supported on a stack of different color, see Fig. 8. The figure shows how X type stabilizer on the red stack and Y type stabilizers on the blue and green stacks can be combined to form the hypercycle stabilizer on green face of TSCC.

$$W_2^{f_r} = (B_{f_r}^Y)_r (B_{f_r}^Y)_g (B_{f_r}^X)_b \quad (12a)$$

$$W_2^{f_g} = (B_{f_g}^X)_r (B_{f_g}^Y)_g (B_{f_g}^Y)_b \quad (12b)$$

$$W_2^{f_b} = (B_{f_b}^Y)_r (B_{f_b}^X)_g (B_{f_b}^Y)_b \quad (12c)$$

Using these decompositions, we can also measure the syndromes of the TSCCs using the color code stabilizer outcomes.

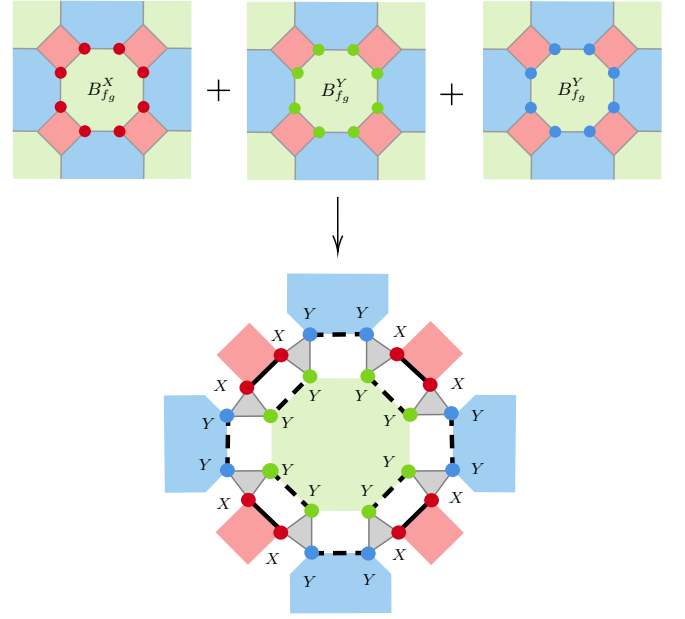


FIG. 8: Decomposition of $W_2^{f_g}$ into the stabilizers on color codes, namely, $(B_{f_g}^X)_r$, $(B_{f_g}^Y)_g$, and $(B_{f_g}^Y)_b$.

Algorithm 1 Syndrome computation for TCC and TSCC

Input: TSCC hypergraph \mathcal{H}_Γ , set of erasure positions \mathcal{E} .

Output: X error syndrome s_c^X and Z error syndrome s_c^Z for the color code on the c -stack and syndromes of TSCC.

- 1: Group the qubits according to color of faces on TSCC.
 - 2: **for** every c -stack, $c \in \{r, g, b\}$ **do**
 - 3: Measure 4-body $(B_{f_r}^Z)_c$ and $(B_{f_r}^X)_c$ stabilizers on TSCC.
 - 4: Measure 8-body $(B_{f_g}^Z)_c$, $(B_{f_g}^X)_c$, $(B_{f_b}^Z)_c$ and $(B_{f_b}^X)_c$ stabilizers on TSCC.
 - 5: **end for**
 - 6: Calculate W_2^f using Eq. (12) for all $f \in F$.
 - 7: Return s_c^Z and s_c^X , $c \in \{r, g, b\}$, syndromes of W_1^f and W_2^f . ▷
- Note that $(B_f^Z)_c = W_1^f$ where $f \in F_c$.
-

B. Preprocessing the TSCC

Algorithm 1 shows how all the color code stabilizer and TSCC stabilizer measurements are obtained. In this section we state how the TSCC syndrome can be used to do preprocessing on the TSCC. We use two preprocessing techniques, clustering and peeling for our algorithms. TSCC syndromes are used during the peeling stage. First, we apply the preprocessing techniques to remove some simple erasure patterns. We update the TCC syndromes when any correction is done during peeling. After peeling we perform clustering of the remaining erasures. For more details, refer [10].

V. FIRST STAGE: X ERROR CORRECTION USING GAUGE FIXING

In this section we study the first stage- bit flip error correction. As shown in Fig. 3, we map the TSCC to three copies of color codes. Since there is one to one correspondence between the qubits of the color codes and the TSCC, we can directly map the erasures on TSCC onto the color codes. Next we obtain the X error syndrome, by measuring Z type stabilizers of the color codes as shown in Fig. 7. Once the syndrome on each stack is obtained, we decode the color code on that stack using a color code erasure decoder and get an error estimate. We adapt the color code erasure decoder proposed in [24]. The final step is to lift the estimate from all the color codes to the TSCC. Since every qubit of the color code is a dedicated TSCC qubit (see Sec. IID), we lift the error estimate at the same location on the TSCC. Note that since no stack share any qubit, all the three color codes can be decoded parallelly and independently.

We also update the hypercycle syndrome W_2^f at the end of this stage. This is done because correcting the X errors clears B_f^Z stabilizers and hence modifies the B_f^Y stabilizers. As shown in Eqn. 12, the hypercycle stabilizer directly depends on both X and Y type color code stabilizers. Hence any modification in the color code stabilizer syndrome also affects the hypercycle syndrome.

The complete decoding procedure for the first stage is given in Algorithm 2 with $\sigma = X$. During this stage of correction, we clear all the Z type stabilizers of the color codes. Note that only a subset of these stabilizers are actually a stabilizer on the TSCC. (Recall that $(B_f^Z)_c = W_1^f$ where $f \in F_c$.) Hence we are fixing additional TSCC gauge operators, on top of TSCC rank-2 stabilizers, while clearing the bit flip errors.

Algorithm 2 TSCC erasure decoder via mapping to TCCs: Bit flip (Phase flip) error correction

Input: TSCC hypergraph \mathcal{H}_Γ , set of erasure positions \mathcal{E} and σ error syndrome $s_c^\sigma, c \in \{r, g, b\}$. \triangleright Note σ can be either X or Z

Output: σ error estimate \hat{E}^σ

- 1: $\hat{E}^\sigma = I$
 - 2: Group the qubits according to color of faces on TSCC.
 - 3: **for** every c -stack, $c \in \{r, g, b\}$ **do**
 - 4: $\hat{E}_c = I$
 - 5: Map erasure locations directly as per the color.
 - 6: Given s_c^σ , decode color code using any color code erasure decoder to get estimate \hat{E}_c .
 - 7: Lift the estimate \hat{E}_c to the subsystem code.
 - 8: Update W_2^f syndrome according to the estimate.
 - 9: Update $\hat{E}^\sigma = \hat{E}^\sigma \hat{E}_c$.
 - 10: **end for**
 - 11: Return \hat{E}_σ as the final σ error estimate.
-

A. Residual errors after correcting bit flip errors

As can be seen from Algorithm 2, we decode the erasure induced bit flip errors by means of a color code erasure decoder.

If the decoder only estimates on the erased qubits, then one can immediately proceed to correct the phase error caused by the erasure. However, in some cases, this decoder can cause a new Z type error on unerased qubits as in the case of [10], see for example Fig. 9. So this must be accounted for in the next stage. In this paper we used the erasure color code decoder proposed in [24]. This particular decoder can potentially return an error estimate on nonerased qubits up to an X type stabilizer or logical operator on the color code. (This is because the decoder works by mapping on to surface codes which can generate additional errors, see [24] for more details.) When the estimate is up to a stabilizer on the color code, on the subsystem code the error is up to an X type gauge operator because X type stabilizers on the color code are gauge operators on the subsystem code. When the estimate is up to a logical operator on the color code, on the subsystem code the error can either be a logical operator or an X type gauge operator.

Suppose a part of the error pattern is as shown in Fig. 10a. Note that support of the error lies only on the red color code, see Fig. 10b. We measure the color code stabilizers directly on the TSCC to obtain the syndrome shown in Fig. 10b. With the syndrome and erased locations, we decode the color code using color code erasure decoder and obtain error estimate as shown in Fig. 10c. Note that the estimate is not same as the original error, but it results in the same syndrome. When we apply this estimate to the original error on the color code, it results in a stabilizer as shown in Fig. 10d. (Therefore, the correction is up to a stabilizer.) When the estimate is lifted to the TSCC, we get a resultant X type gauge operator, shown in Fig. 10e. This example shows that the final outcome can induce an X type gauge error but not any additional Z errors on the unerased qubits. The following lemma proves this result formally.

Lemma 3. *On performing X error correction on a TSCC by decoding on three copies of color codes through Algorithm 2, the lifted error estimate can either be an X type gauge operator or a logical operator (bare or dressed). If the estimate on the color codes is up to a stabilizer, then the lifted error estimate does not contain any Z error on the unerased qubits.*

Proof. Suppose that the X part of the error on the TSCC is denoted E and its restriction to the color code on c -stack be E_c . Let the error estimate returned by Algorithm 2 be \hat{E}_c on the color code on the c -stack. This estimate can be decomposed as $\hat{E}_c = E_c L S$, where L is a logical operator and S is a stabilizer of the color code. This estimate will be a pure X type operator on the color code as it is a CSS code. When \hat{E}_c is equal to E , we get a perfect correction step and there is no residual error on the color code or the TSCC. If \hat{E}_c is not equal to E , the estimate is up to a X stabilizer or a logical operator. When this estimate is lifted to the TSCC, it can either be a logical operator or a pure X type gauge operator. If the estimate is up to a (nontrivial) logical operator on the color codes, then from Eq. (2), we see that the lifted error estimate on the subsystem code, is an X type gauge operator or a dressed logical operator of the subsystem code. Recall that a dressed logical operator is a logical operator of the TSCC augmented with additional gauge generators.

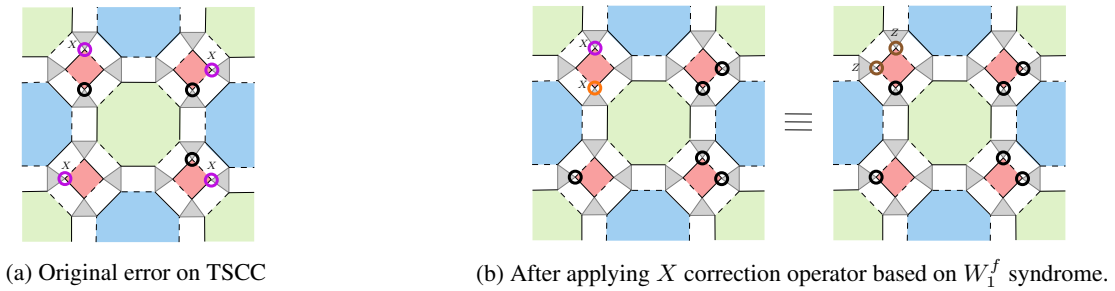


FIG. 9: Fig. 9a shows the original error on TSCC. The purple rings denote erased locations with X error and black rings denote erased locations with identity. On performing bit flip correction as per [10], the resultant TSCC is shown in Fig. 9b. The orange ring denotes the X error estimate and brown ring denotes Z error. As highlighted with green net patterned circle, there exists a residual Z error on unerased qubit as well.

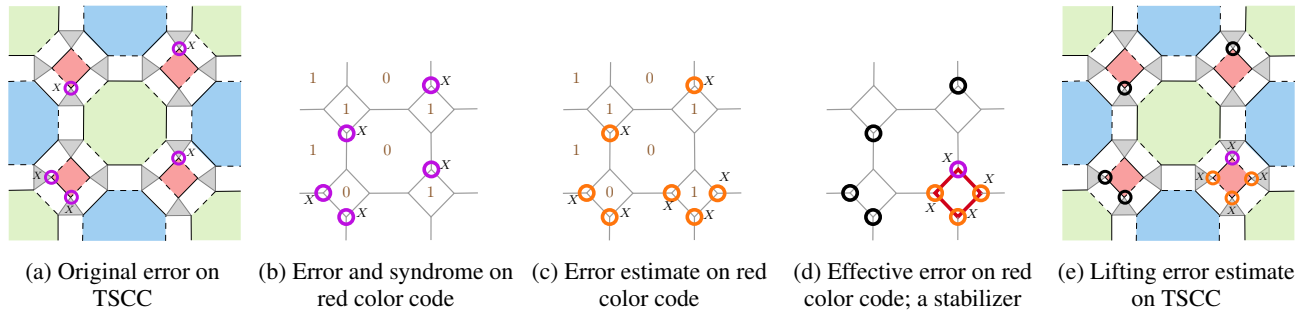


FIG. 10: Original error on TSCC is shown in Fig. 10a. Purple rings denote the erased locations with X error. Fig. 10b shows the error and syndrome on the red color code. In Fig. 10c, orange ring denote the X error estimate on red color code. Fig. 10d shows the error + error estimate on red color code. As highlighted with red, the resultant is a color code stabilizer. Fig. 10e shows how after applying the color code estimate we get resultant X type gauge operator.

In case the estimate is up to a stabilizer on the color codes, then on the subsystem code, the estimate is up to an X type gauge operator that does not contain any Z errors on the unerased qubits. This is because the (X type) stabilizers of the color codes on each stack are in the gauge group. \square

Lemma 3 shows that the lifted estimate on the TSCC does not result in any nonzero syndrome on the TSCC, therefore the second stage can also focus only on the erased qubits and ignore the unerased qubits.

Note that when the decoders on the color codes fail, it does not always lead to logical error on the TSCC as well. The following example illustrates this. Consider now the same error pattern as Fig. 9a this time decoded using Algorithm 2. For simplicity we choose an error pattern which is supported only on the red faces, Fig. 11a shows the error. Fig. 11b shows the error pattern and the corresponding syndrome on the red stack. Suppose the decoder results in the estimate shown in Fig. 11c. On correcting according to this estimate, the resultant operator is a logical operator on the color code as shown in Fig. 11d. When the estimate shown in Fig. 11c is lifted to the TSCC, we get an X type gauge operator as shown in Fig. 11e. Estimate on color code up to a logical error can result to an X type gauge operator on the TSCC or a dressed logical operator on TSCC. In either case it does not create any additional Z error syndrome on the TSCC.

Before we conclude this section, in Table I we summarize the differences between the bit flip error decoding in Ref. [10] and Algorithm 2.

Parameters	Ref. [10]	Algorithm 2
Type of decoding	Local	Global
X error correction on	TSCC	Three copies of color codes
Error estimate on each face	Single X error	One or more X errors
Error estimate	Can create residual Z error on unerased qubits	Estimate is a X type gauge operator or logical operator

TABLE I: Differences between first stage (bit flip error correction) of Ref. [10] decoder and proposed decoder

VI. SECOND STAGE: Z ERROR CORRECTION

After performing X error correction, the next step is to correct the Z errors. We corrected the X errors with gauge fixing since we also fixed additional TCC stabilizers apart from TSCC stabilizers. In this section, we propose two algorithms to correct the Z errors. One of them uses only the stabilizers

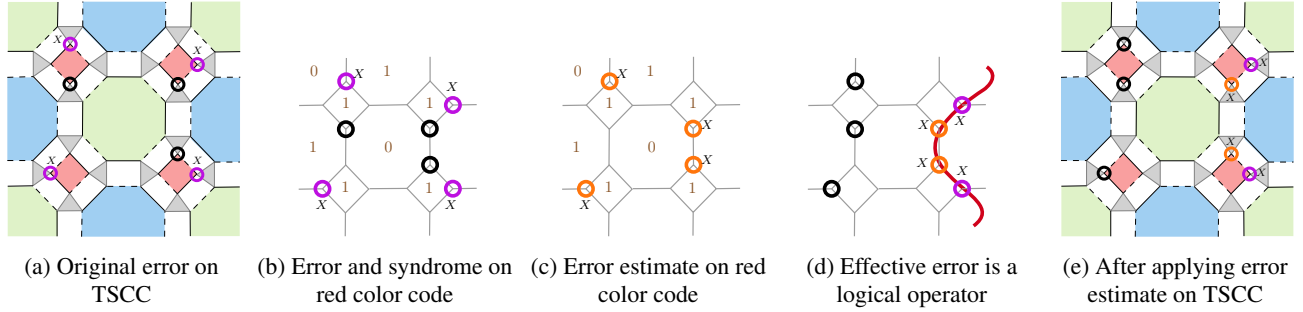


FIG. 11: The original error on TSCC is shown in Fig. 11a (same as Fig. 9a). Fig. 11b shows the error and syndrome on color code on red stack. In Fig. 11c, orange ring denote the X error estimate. Fig. 11d shows the error + error estimate on the color code. Fig. 11e shows how after applying the color code estimate we get resultant X type gauge operator.

of the TSCC while the other uses the TCC X type stabilizers.

A. Correcting Z errors without gauge fixing

Recall that the TSCC is constructed from a 2-colex using vertex expansion. For Z error correction, we take the hypercycle syndromes of the TSCC and map them onto the parent 2-colex Γ from which the TSCC is derived. For face f , the hypercycle syndrome W_2^f corresponds to the X type stabilizer syndrome of the corresponding face on the 2-colex Γ . Since we have already cleared the X errors in the first stage, the residual syndrome on the lattice due to hypercycle stabilizers can be explained purely in terms of Z errors alone. Next we also map the erasures from the TSCC to the parent 2-colex. A vertex of the 2-colex is erased if any one or more qubits of the hyperedge (inflated triangle) in the TSCC are erased. The syndromes of the hypercycles are projected to the 2-colex. (Note that the hypercycle syndromes were updated after performing X error correction.) Once the erased locations and syndromes are obtained on the underlying color code, we can adapt any color code erasure decoder to decode it.

After decoding, we lift the error estimate on the TSCC. A Z error estimate on a color code qubit is lifted to Z error on any one of the qubits on the corresponding hyperedge in the TSCC. The complete procedure for Z error correction is given in Algorithm 3.

Algorithm 3 Correcting Z errors without gauge fixing

Input: TSCC hypergraph \mathcal{H}_Γ , erasure positions \mathcal{E} and syndrome of hypercycle stabilizers (W_2^f).

Output: Z Error estimate \hat{E}^Z

- 1: Project the updated W_2^f syndromes (from Algorithm 2) to the underlying parent color code of the TSCC.
 - 2: Map the erasure locations.
 - 3: Adapt any color code erasure decoder to obtain an error estimate \bar{E} (on the color code).
 - 4: Lift the error estimate \bar{E} to the TSCC. Denote the lifted estimate \hat{E}^Z .
 - 5: Return \hat{E}^Z as the error estimate for Z errors.
-

We summarize the entire decoding algorithm. We use Algo-

rihm 1 to compute the syndrome for decoding. We incorporate preprocessing techniques like peeling and clustering for better performance as in [10]. After performing the preprocessing steps, we decode the bit flip errors using Algorithm 2, for the first stage of decoding. In the next stage we decode the phase flip errors using Algorithm 3. The complete algorithm is given in Algorithm 4. The performance of this decoder is shown in Fig. 13. We obtain a threshold of about 17.7%.

Remark 4. For correcting the X errors we fix, in effect, $3|F| - 6$ independent commuting operators from the gauge group and $|F| - 2$ commuting operators for correcting the Z errors. Thus a total of $4|F| - 8$ commuting gauge operators are fixed. The TSCC would have measured only $2|F| - 2$ operators. Thus by partial gauge fixing we are fixing an additional $2|F| - 6$ gauge operators as checks.

Recall from Remark 1, that the gauge group of the TSCC is generated by $2r + s = 10|F| - 2$ operators where $s = 2|F| - 2$ is the number of independent stabilizer generators of the subsystem code and $r = 4|F|$ is the number of gauge qubits. The maximal commuting subgroup in the gauge group is of size $r + s = 6|F| - 2$. Since we measured only $4|F| - 8$ checks we see that this decoder is a partial gauge fixing algorithm.

Observe that in this decoder, the erasure induced X errors are corrected using gauge fixing while the Z errors are not. This naturally suggests the design of a decoder that fixes more gauge operators. We take this up in the next section.

B. Correcting Z errors with gauge fixing

In Section VIA we discussed an algorithm which uses partial gauge fixing to decode TSCC. In partial gauge fixing we perform gauge fixing for clearing only bit flip errors. The phase flip errors are cleared by decoding the parent color code. The improvement in the threshold performance prompts us to fix additional gauge generators. We now explore the correction of Z errors by gauge fixing. In partial gauge fixing, we fixed $4|F| - 8$ gauge operators out of the maximal commuting subgroup of $6|F| - 2$. Hence there is a scope of fixing $2|F| + 6$ additional gauge operators on TSCC. In this section we correct phase flip errors with gauge fixing, similar to bit

flip error correction. We map the TSCC on to three copies of color codes and decode them for correcting phase flip errors.

We obtain syndromes for X type stabilizers of the color codes using Algorithm 1. Once the color code syndromes are obtained, we decode the color codes by adapting a color code erasure decoder. We then lift the joint estimate on all the stacks back to the TSCC. We lift the error estimate back on the TSCC according to the color of the color code. Considering we clear both X and Z error on the copies of color codes, we perform gauge fixing for correcting both the errors. We use Algorithm 2, with $\sigma = Z$, to correct phase flip errors with gauge fixing.

Remark 5. *We can see that in effect we are fixing $6|F| - 12$ independent stabilizers. On TSCC it is possible to gauge fix at most $r + s = 6|F| - 2$ stabilizers. Compared to the TSCC where we measure $2|F| - 2$ stabilizers we are measuring in addition $4|F| - 10$ gauge operators. Thus we are order maximal with respect to the number of gauge operators that are being fixed.*

From Eq. (12), we have that the hypercycle stabilizer of TSCC can be decomposed to a sum of color code stabilizers. Therefore, clearing the syndromes on the color codes also clears the syndrome on the TSCC. This makes sure that correction restores the state to the codespace, namely, the joint $+1$ -eigenspace of the subsystem code stabilizers. (Since color code is a CSS code, we can perform X error correction and Z error correction in any order.)

C. Complete algorithm

In this section we summarize both the X and Z correction for both approaches. The complete algorithm is given in Algorithm 4. The first step is to obtain the necessary syndromes for decoding the TSCC. Along with the syndromes of the color codes, we also compute the syndrome of the TSCC which helps in the preprocessing using peeling.

The second step is to preprocess using peeling, see refer Algorithm 2 in [10] for further details on peeling. During peeling we correct single isolated erasures using TSCC stabilizer measurements. Peeling results in removal of some erasures and also updates syndromes of some of the stabilizers of the TSCC and the color codes. Based on the location of the erasure where the correction is applied, we modify the color code syndromes as per the stack it belongs to. An erased qubit belonging to a face $f \in F_c$ of TSCC modifies only syndromes of color code on c -stack. We also update the hypercycle stabilizer syndromes. Every qubit participates in three hypercycles. Hence syndrome of these hypercycle stabilizers must be modified based on the error estimate. For simulation simplicity we re-compute hypercycle stabilizers after every correction step during peeling. They are used for phase flip error correction during partial gauge fixing decoding. We do need not to keep track of the hypercycle syndromes for the order maximal gauge fixing decoder since we do not utilize them for further error correction.

After peeling, some of the erasures are corrected and the syndromes appropriately modified. Peeling is followed by clustering of erasures. We scan the lattice from left to right and top to bottom and search for a stabilizer which contains at least one erased qubit. We group the erased qubits of the stabilizer to form a cluster. (This is true even if there is a single erasure in that stabilizer.) For each of the erased qubit we check if it is already part of a previously formed cluster. If so, we merge these clusters. We repeat this procedure for every stabilizer. At the end, erasures of two distinct clusters do not participate in a common stabilizer. For more details on clustering, see [10].

Once the clusters are formed, the next step is to decode every cluster independently. For every cluster, we perform bit flip error correction using Algorithm 1. We then correct the phase flip errors. If decoding with partial gauge fixing decoder, we use Algorithm 3 and for order maximal gauge fixing decoder, we use Algorithm 1. All error estimates for each of the clusters are combined and returned at the end of the algorithm. Note that for order maximal gauge fixing since both bit flip error syndrome and phase flip error syndrome do not affect each other, we can decode both these errors in parallel.

Algorithm 4 Erasure decoder for TSCC

Input: TSCC hypergraph \mathcal{H}_Γ , set of erasure positions \mathcal{E} and choice of decoding: partial gauge fixing decoding or order maximal gauge fixing decoding.

Output: Error estimate \hat{E}

- 1: $\hat{E} = I$.
 - 2: Use Algorithm 1 to obtain syndrome s_c^σ , $\sigma \in \{X, Z\}$, $c \in \{r, g, b\}$ and syndromes of W_1^f and W_2^f for all $f \in F$.
 - 3: Perform peeling to obtain correction operator \hat{E}_p , refer [10].
 - 4: Update the color code and TSCC stabilizers and the list of erasures.
 - 5: Cluster remaining erasures which share a stabilizer. \triangleright Let the number of clusters be n_c .
 - 6: **if** $1 \leq i \leq n_c$ **then**
 - 7: Use Algorithm 2, with $\sigma = X$, to obtain X error estimate \hat{E}^X .
 - 8: **if** partial gauge fixing decoder **then**
 - 9: Use Algorithm 3 to obtain Z error estimate \hat{E}^Z .
 - 10: **else**
 - 11: Use Algorithm 2, with $\sigma = Z$, to obtain Z error estimate \hat{E}^Z .
 - 12: **end if**
 - 13: $\hat{E} = \hat{E} \hat{E}^X \hat{E}^Z$
 - 14: **end if**
 - 15: Return $\hat{E} \hat{E}_p$ as the final error estimate.
-

We obtained a threshold of 44% for the order maximal gauge fixing decoder, shown in Fig. 14. Note that for both the decoding algorithms we are measuring all the color code stabilizers. The main difference between the two algorithms is the count of gauge operators fixed. Another crucial difference is the number of times the color code erasure decoder needs to be executed for each of the decoders. In Table II we highlight the key differences between the decoders. We discuss the simulation results in Section VIII. Before that, we

study the correctability of erasure patterns on TSCCs in the next section.

VII. CORRECTABILITY CONDITION ON ERASURE PATTERN

In this section we propose correctability conditions for an erasure pattern on subsystem codes. Using the correctability condition we can test, prior to decoding, whether an erasure pattern can be corrected or not. In Theorem 6, we propose the condition for a general subsystem code.

Before we begin, we introduce a few notations necessary for this section. We denote the stabilizer matrix of the subsystem code by H and matrix representation of the gauge group over \mathbb{F}_2 by G . The stabilizer matrix H involves all the (independent) stabilizer generators of the subsystem code while G consists of the gauge generators. Let $H_{\mathcal{E}}$ be a submatrix which is a restriction of H to the subset of columns corresponding to locations of erased qubits. Similarly, we denote by $G_{\mathcal{E}}$ and $\mathcal{E}_{\bar{\mathcal{E}}}$, the submatrices of G restricted to the qubits in \mathcal{E} and $\bar{\mathcal{E}}$ respectively. The submatrix $H_{\bar{\mathcal{E}}}$ consists of the remaining columns of H . We denote the stabilizer matrix of the parent color code by H_c , where $c \in \{r, g, b\}$.

An erasure pattern \mathcal{E} is correctable if all the errors supported in \mathcal{E} are correctable and non-correctable otherwise. Equivalently, if \mathcal{E} supports a logical error, then it is not correctable and correctable otherwise. A necessary condition for an erasure pattern to be correctable for stabilizer codes due to [21] is as follows:

Proposition 1 ([21]). *For stabilizer codes, an erasure pattern \mathcal{E} is correctable only if*

$$2|\mathcal{E}| \leq \text{rank}(H) + \text{rank}(H_{\mathcal{E}}) - \text{rank}(H_{\bar{\mathcal{E}}}) \quad (13)$$

Proposition 1 immediately gives a sufficient condition for a correctable erasure pattern decoded via order maximal gauge fixing decoder. Specifically, if Eq. (13) is satisfied on all the three copies of color code i.e.,

$$2|\mathcal{E}_c| \leq \text{rank}(H_c) + \text{rank}(H_{\mathcal{E}_c}) - \text{rank}(H_{\bar{\mathcal{E}}_c}) \quad (14)$$

for every c , where $c \in \{r, g, b\}$, then the erasure is correctable by the order maximal gauge fixing decoder. Note that this is only a sufficient condition for the correctability of an erasure pattern and not a necessary condition, see the discussion in Section V A.

We now propose a condition for correctable erasures applicable to general subsystem codes decoded without gauge fixing. This condition also accounts for the gauge group.

Theorem 6 (Correctable erasures on a subsystem code without gauge fixing). *An erasure pattern \mathcal{E} on a TSCC is correctable only if the following condition is satisfied.*

$$2|\mathcal{E}| = \text{rank}(H_{\mathcal{E}}) + \text{rank}(G) - \text{rank}(G_{\bar{\mathcal{E}}}) \quad (15)$$

Proof. Up to a phase, there are $4^{|\mathcal{E}|}$ Pauli errors that can be supported in \mathcal{E} . There are $2^{\text{rank}(H_{\mathcal{E}})}$ syndromes possible. For

each syndrome there exist $2^{2|\mathcal{E}| - \text{rank}(H_{\mathcal{E}})}$ error patterns. Consider the map

$$\pi_{\bar{\mathcal{E}}} : G \rightarrow G_{\bar{\mathcal{E}}} \quad (16)$$

The operators in the kernel of $\pi_{\bar{\mathcal{E}}}$ are exactly the operators in G whose support is entirely in \mathcal{E} . The dimension of $\ker \pi_{\bar{\mathcal{E}}}$ is given by

$$\ker(\pi_{\bar{\mathcal{E}}}) = \text{rank}(G) - \text{rank}(G_{\bar{\mathcal{E}}}) \quad (17)$$

All errors in $\ker(\pi_{\bar{\mathcal{E}}})$ have support only in \mathcal{E} and have zero syndrome. First observe that such errors cannot be more than the total number of errors supported in \mathcal{E} which have zero syndrome. Therefore, $\text{rank}(G) - \text{rank}(G_{\bar{\mathcal{E}}}) \leq 2|\mathcal{E}| - \text{rank}(H_{\mathcal{E}})$. If errors in $\ker(\pi_{\bar{\mathcal{E}}})$ are fewer than the number of distinct errors with the same syndrome, then \mathcal{E} supports nontrivial logical error(s). Therefore, if $\text{rank}(G) - \text{rank}(G_{\bar{\mathcal{E}}}) < 2|\mathcal{E}| - \text{rank}(H_{\mathcal{E}})$, then \mathcal{E} is not correctable. If $2|\mathcal{E}| - \text{rank}(H_{\mathcal{E}}) = \text{rank}(G) - \text{rank}(G_{\bar{\mathcal{E}}})$, all such errors are in the gauge group. So \mathcal{E} does not support a (nontrivial) logical operator and \mathcal{E} is a correctable erasure pattern. \square

Remark 7. *Since it is not possible for $\text{rank}(G) - \text{rank}(G_{\bar{\mathcal{E}}}) > 2|\mathcal{E}| - \text{rank}(H_{\mathcal{E}})$, we can state the correctability condition in Theorem 6 slightly differently. More precisely, an erasure is correctable only if*

$$2|\mathcal{E}| \leq \text{rank}(H_{\mathcal{E}}) + \text{rank}(G) - \text{rank}(G_{\bar{\mathcal{E}}}) \quad (18)$$

In this form it reduces to the condition in [21, Eq. (4)], when G is Abelian i.e., we have a stabilizer code.

We performed simulations based on the condition in Eq. (15). We generate an erasure pattern \mathcal{E} where qubit is erased with a probability ε on the subsystem code. As per the locations of \mathcal{E} , we compute the rank of the matrices $H_{\mathcal{E}}$ and $G_{\bar{\mathcal{E}}}$. Rank of G remains constant throughout the simulations since it is independent of \mathcal{E} . If the condition in Eq. (15) gets violated, we flag it as an uncorrectable error. We repeated the experiment for 10000 trials for various ε for code distances $d = 4, 8, 16$. We obtained a threshold of approximately 16.5% as shown in Fig. 12.

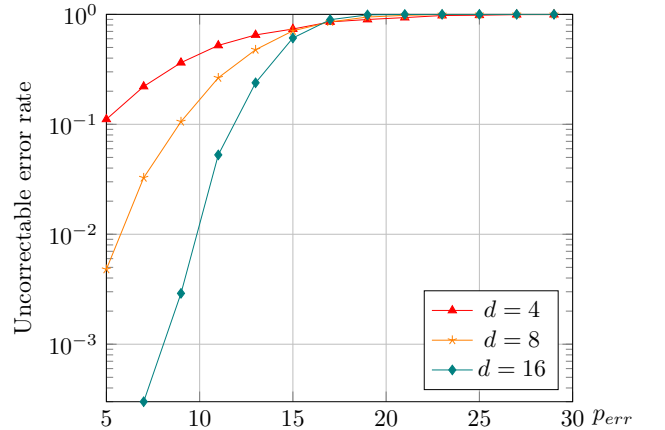


FIG. 12: Threshold of $\approx 16.5\%$ based on Eq. (15).

Decoder	Partial gauge fixing decoder	Maximal gauge fixing decoder
Lattice for X error correction	Three copies of (parent) color code of the TSCC.	
X error correction	Map erasures and syndrome to three copies of color codes. Decode them using an erasure decoder.	
Lattice for Z error correction	Parent color code of TSCC	Three copies of (parent) color code
Z error correction	Map W_2^J syndrome and erased locations to the parent color code. Decode using an erasure decoder	Map erasures and syndrome to three copies of color codes. Decode them using an erasure decoder.
Number of commuting gauge operators fixed	$4 F - 8$	$6 F - 12$
Number of times color code erasure decoder is utilized	4	6
Errors for which gauge fixing is used	Only X errors	Both X and Z errors
Threshold	17.7%	44%

TABLE II: Comparison between partial gauge fixing decoder and order maximal gauge fixing decoder.

VIII. SIMULATION RESULTS

In this section we present the simulation results for both the decoding algorithms. We simulate for the TSCC derived from square octagon lattice. The proposed algorithms can be easily adapted to other TSCCs.

A. Simulation setup

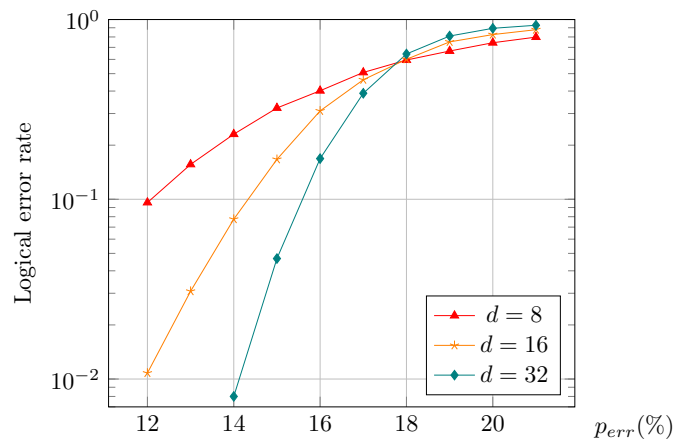
An erasure pattern is generated on the subsystem codes according to the probability of erasure ε . Noise on each qubit is assumed to be identical and independent. Then using the erasure model described in Section II E, we generate Pauli errors on each of the erased qubits with equal probability. Every erased location can undergo any of the Pauli errors with equal probability as described in Section II E. Then we correct these induced Pauli errors on the subsystem code. We use Algorithm 4 for decoding.

In practice, while decoding a subsystem code, its stabilizers are measured indirectly via measuring the gauge generators and classically combining the outcomes appropriately. The proposed decoders map the TSCCs to multiple copies of color codes in order to decode them. We measure the multi-body color code stabilizers *directly* on the TSCC. Once the color code stabilizers are measured, we decode the three copies of color code using the color code erasure decoder [24]. This decoder only needs the erasure locations as input and generates its own syndrome. We adapted it so that takes as input the previously measured syndrome and the erasure locations.

After decoding the color code copies, we lift the estimate to TSCC. After lifting we check if any logical error has occurred or not. If the product of original error and the error estimate anticommutes with any one of the bare logical operators, we declare a logical error.

B. Results

We present the simulation results for the TSCC derived from square octagon lattice. The TSCCs derived from the square octagon lattices have the code parameters $[[3d^2, 2, 2d^2, d]]$, where d is the distance of the code [17, 28]. We have simulated the proposed decoders for these codes for various erasure probabilities and lattice sizes. The gauge measurements are assumed to be noiseless. The plots shown in Fig. 13 and Fig. 14 show the variation of logical error rate with respect to the probability of erasure errors. A logical error occurs when the error and error estimate differ by a non-trivial logical operator of the TSCC. Every data point has been obtained by accumulating 2000 logical errors or 10000 runs, whichever occurs earlier.

FIG. 13: Performance of partial gauge fixing decoder. Threshold is $\approx 17.7\%$.

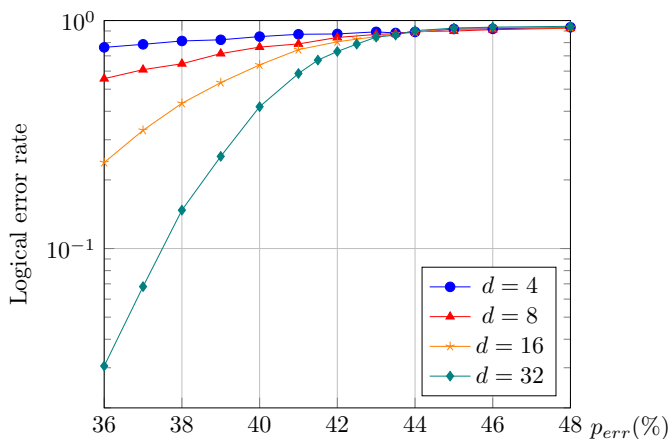


FIG. 14: Performance of the order maximal gauge fixing decoder. Threshold is $\approx 44\%$.

Fig. 13 shows the plot for performance of the partial gauge fixing decoder. We report a threshold of approximately 17.7%. This suggests that gauge fixing improves the performance in comparison to the highest threshold of 9.7% given in [10]. When extending to almost full gauge fixing, we observe a threshold of 44% as shown in Fig. 14. The performance of our decoder is close to 50% which is set by the no-cloning theorem.

IX. CONCLUSION

In this paper, we proposed two algorithms for decoding subsystem codes over erasure channel. By using the technique of gauge fixing in combination with other preprocessing techniques we were able to significantly improve the threshold of TSCCs for the erasure noise with respect to our previous work [10]. Our work draws upon the mapping of TSCC to multiple copies of color codes proposed in [4]. We decode on these color codes instead of decoding directly on TSCC which motivates in a sense the need for gauge fixing. Our first decoder uses partial gauge fixing where gauge fixing is used only to correct erasure induced bit flip errors. The second decoder uses maximal gauge fixing where both bit flip and phase flip errors are corrected via gauge fixing. The later decoder gives us a threshold of 44%. To the best of our knowledge, this is the highest threshold to date for a TSSC for erasure noise. Syndrome measurement for both the decoders requires us to measure 4-body and 8-body measurements. We also formulated conditions for correctability of erasures on the subsystem codes. There remain many other interesting open questions in this context. Developing an optimal decoder without gauge fixing, improving the performance of the proposed decoders, reducing the complexity of syndrome measurement are some natural problems for further study.

Acknowledgment. HMS would like to thank Arun B. Alosious for valuable discussions.

-
- [1] D. Bacon, Operator quantum error-correcting subsystems for self-correcting quantum memories, *Phys. Rev. A* **73**, 012340 (2006).
 - [2] D. W. Kribs, R. Laflamme, and D. Poulin, Unified and generalized approach to quantum error correction, *Phys. Rev. Lett.* **94** (2005).
 - [3] D. Poulin, Stabilizer formalism for operator quantum error correction, *Phys. Rev. Lett.* **95**, 230504 (2005).
 - [4] H. Bombin, G. Duclos-Cianci, and D. Poulin, Universal topological phase of two-dimensional stabilizer codes, *New J. of Physics* **14**, 073048 (2012).
 - [5] M. Suchara, S. Bravyi, and B. Terhal, Constructions and noise threshold of topological subsystem codes, *Journal of Physics A: Mathematical and Theoretical* **44**, 155301 (2011).
 - [6] V. V. Gayatri and P. K. Sarvepalli, Decoding topological subsystem color codes and generalized subsystem surface codes, in *2018 IEEE Information Theory Workshop (ITW)* (IEEE, 2018) pp. 1–5, Extended version arXiv:1805.12542.
 - [7] O. Higgott and N. P. Breuckmann, Subsystem codes with high thresholds by gauge fixing and reduced qubit overhead, *Physical Review X* **11**, 031039 (2021).
 - [8] N. C. Brown, M. Newman, and K. R. Brown, Handling leakage with subsystem codes, *New J. of Physics* **21**, 073055 (2019).
 - [9] M. Grassl, T. Beth, and T. Pellizzari, Codes for the quantum erasure channel, *Phys. Rev. A* **56**, 33 (1997).
 - [10] H. Solanki and P. K. Sarvepalli, Correcting erasures with topological subsystem color codes, in *2020 IEEE Information Theory Workshop (ITW) (ITW-20)* (Riva del Garda, Italy, 2021).
 - [11] R. S. Andrist, H. Bombin, H. G. Katzgraber, and M. A. Martin-Delgado, Optimal error correction in topological subsystem codes, *Phys. Rev. A* **85**, 050302 (2012).
 - [12] A. Paetznick and B. W. Reichardt, Universal fault-tolerant quantum computation with only transversal gates and error correction, *Phys. Rev. Lett.* **111**, 090505 (2013).
 - [13] H. Bombin, Gauge color codes: optimal transversal gates and gauge fixing in topological stabilizer codes, *New J. of Physics* **17**, 083002 (2015).
 - [14] M. A. Nielsen and I. L. Chuang, *Quantum Computation and Quantum Information* (Cambridge University Press, 2010).
 - [15] T. A. B. Daniel A. Lidar, *Quantum Error Correction* (Cambridge University Press, 2013).
 - [16] H. Bombin and M. A. Martin-Delgado, Topological quantum distillation, *Phys. Rev. Lett.* **97**, 180501 (2006).
 - [17] H. Bombin, Topological subsystem codes, *Phys. Rev. A* **81**, 032301 (2010).
 - [18] A. J. Moncy and P. K. Sarvepalli, Performance of nonbinary cubic codes, in *2018 International Symposium on Information Theory and Its Applications (ISITA)* (IEEE, 2018) pp. 334–338.
 - [19] A. Kulkarni and P. K. Sarvepalli, Decoding the three-dimensional toric codes and welded codes on cubic lattices, *Phys. Rev. A* **100**, 012311 (2019).
 - [20] N. Delfosse and G. Zémor, Linear-time maximum likelihood decoding of surface codes over the quantum erasure channel, *Phys. Rev. Research* **2**, 033042 (2020).
 - [21] N. Delfosse and G. Zémor, Upper bounds on the rate of low density stabilizer codes for the quantum erasure channel, arXiv:1205.7036 (2012).
 - [22] C. Vuillot, L. Lao, B. Criger, C. G. Almudéver, K. Bertels, and

- B. M. Terhal, Code deformation and lattice surgery are gauge fixing, *New J. of Physics* **21**, 033028 (2019).
- [23] H. P. Nautrup, N. Friis, and H. J. Briegel, Fault-tolerant interface between quantum memories and quantum processors, *Nature communications* **8**, 1 (2017).
- [24] A. B. Alosious and P. K. Sarvepalli, Erasure decoding of two-dimensional color codes, *Phys. Rev. A* **100**, 042312 (2019).
- [25] J. Haah, Algebraic methods for quantum codes on lattices, *Revista colombiana de matematicas* **50**, 299 (2016).
- [26] N. Delfosse, Decoding color codes by projection onto surface codes, *Phys. Rev. A* **89**, 012317 (2014).
- [27] We would like to acknowledge Oscar Higgot for highlighting this issue in the previous version of this paper.
- [28] P. Sarvepalli and K. R. Brown, Topological subsystem codes from graphs and hypergraphs, *Phys. Rev. A* **86**, 042336 (2012).